

# Flow profile measurement in microchannel using the Optical Feedback Interferometry sensing technique

Lucie Campagnolo · Milan Nikolić · Julien Perchoux · Yah Leng Lim ·  
Karl Bertling · Karine Loubière · Laurent Prat · Aleksandar D. Rakić ·  
Thierry Bosch

Received: date / Accepted: date

**Abstract** The need to accurately measure flow profiles in microfluidic channels is well recognised. In this work, we present a new optical feedback interferometry (OFI) flow sensor that accurately measures local velocity in fluids and enables reconstruction of a velocity profile inside a microchannel. OFI is a self-aligned interferometric technique that uses the laser as both the transmitter and the receiver thus offering high sensitivity, fast response, and a simple and compact optical design. The system described here is based on a commercial semiconductor laser and has been designed to achieve a micrometer range spatial resolution. The sensor performance was validated by reconstructing the velocity profile inside a circular cross-section flow channel with 320  $\mu\text{m}$  internal diameter, with a relative error smaller than 1.8 %. The local flow velocity is directly measured, thus avoiding the need for model based profile calculation and uncertainties inherent to this approach. The system was validated by successfully extracting the flow profiles in both Newtonian and Non-Newtonian liquids.

**Keywords** Photonic device · Laser sensor · Optical feedback interferometry · Flow profile measurement

**PACS** PACS code1 · PACS code2 · more

---

L. Campagnolo · J. Perchoux · T. Bosch  
CNRS, LAAS, 7 avenue du colonel Roche, F-31400 Toulouse, France  
Univ de Toulouse, INPT, LAAS, F-31400 Toulouse, France  
Tel.: +33-5 34 32 25 79  
Fax: +33-5 34 32 25 68  
E-mail: lucie.campagnolo@alumni.enseiht.fr

M. Nikolić · Y.L. Lim · K. Bertling · A.D. Rakić  
The University of Queensland, School of Information Technology and  
Electrical Engineering, Qld 4072, Australia

L. Prat · K. Loubière  
CNRS, Laboratoire de Génie chimique (LGC UMR 5503), F-31432  
Toulouse, France  
Université de Toulouse, INPT, ENSIACET, 4 allée Emile Monso, BP  
84234, F-31432 Toulouse, France

## 1 Introduction

There has been a growing interest to develop microscale devices that can manipulate and transport small amounts of fluid, such as microreactors, micromixers, and lab-on-chip devices. Miniaturization and integration of chemical operations have many specific advantages such as increased speed, efficiency, portability and reduction of reagent consumption (Anxionnaz et al., 2008). Indeed, decreasing device size allows a reduction of technology constraints to the benefit of chemistry (de Mello and Wooton, 2002; Ahmed et al., 2006). This has created a need for new diagnostic tools with spatial resolution in the order of several micrometers. Accurate measurement of velocity distribution in miniature channels is of great interest to provide better understanding of fluidic transport, mixing and fluid properties. Currently, particle imaging velocimetry (PIV) is the most advanced technique for obtaining accurate measurement of velocity distribution in sub-millimeter channels (Meinhart et al., 1999; Santiago et al., 1998; Sarrazin et al., 2006). However, this kind of sensing technology is extremely complex, expensive and bulky.

Optical Feedback Interferometry (OFI) (Bosch et al., 2006) offers a rapid, direct, non-invasive and high-resolution alternative for determining flow rate within flow-channels (de Mul et al., 1992). This technique allows the laser itself to function as both the light source and the detector, making possible low-cost and compact sensors. A number of preliminary applications to flow rate measurement have been previously reported (Zakian et al., 2005; Norgia et al., 2010) and recently measurement of flow in microchannels has been demonstrated (Kliese et al., 2010).

In this study a flow sensor based on OFI is presented that accurately measures the fluid flow profile in sub-millimeter channels. It employs a low-cost Vertical-Cavity Surface-Emitting Laser (VCSEL), a simple 2-lens optical setup and senses

fluid flow rate by monitoring the change in the laser's terminal voltage (Lim et al., 2009). This sensor has been designed to operate in the single scattering regime, that is of interest for a number of chemical and biomedical applications (Norgia et al., 2012).

The aims of this paper are: (i) to present the theory of OFI for fluid flow-rate measurement, (ii) to demonstrate the performance of an OFI flow sensor that measures local velocity in fluids with spatial resolution in the micrometer range and enables reconstruction of a velocity profile inside a microchannel, (iii) to validate the performance of the sensor with deterministic flows that can be easily described with classical analytical solutions.

In Sec. 2., OFI theory applied to fluid flow rate measurement for the single scattering regime is briefly discussed. A detailed description of the experimental set-up is given in Sec. 3. Section 4 presents the experimental results, highlighting the accuracy and the repeatability of the sensor for velocity profile measurement for both Newtonian and non-Newtonian fluids in a circular microchannel. Finally, conclusions are drawn in Sec. 5.

## 2 OFI applied to fluid flow rate measurement

The optical feedback effect occurs when a portion of the light emitted from a laser is reflected from an external target and re-enters the laser cavity (Kane and Shore, 2005). This optical feedback causes measurable changes in the laser frequency and emitted power (Giuliani et al., 2002). The effect can also be observed by monitoring the change in the laser terminal voltage, allowing velocity, distance or displacement measurement (Lim et al., 2009, 2010).

When a laser illuminates an object moving with a velocity  $V_{\text{target}}$ , the reflected optical wave experiences a Doppler shift in frequency. The difference frequency,  $f_{\text{Doppler}}$  is usually referred to as the Doppler frequency (Albrecht et al., 2003; de Groot and Gallatin, 1989):

$$f_{\text{Doppler}} = \frac{2nV_{\text{target}} \cos(\theta)}{\lambda} \quad (1)$$

where  $\theta$  is the angle the target velocity vector makes with respect to the propagation axis of the laser beam,  $\lambda$  is the laser wavelength in free-space and  $n$  the refractive index of the surrounding medium. The Doppler signal is acquired through variations in laser terminal voltage and will be referred to as the OFI signal.

Measuring the flow rate of a moving fluid is similar to measuring the velocity of a solid object. Light emitted from the laser is focused into the fluid by an optical system therefore defining the sensing volume from where the signal is being obtained. Light scattered from a single moving particle that is suspended in the fluid, is shifted in frequency by the Doppler effect, Eq. (1). The optical system collects light

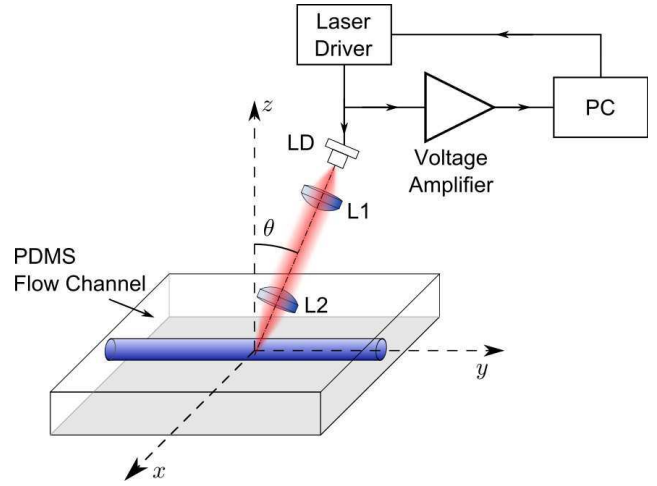


Fig. 1 Experimental setup

back-scattered from a number of different particles with different velocities, leading to a distribution of Doppler frequencies in the OFI signal spectrum instead of a single beat frequency peak. For a liquid where the particle concentration is low enough that multiple scattering can be ignored, a peak appears in the frequency spectrum corresponding to the mean Doppler frequency of the moving particles within the sensing volume.

In OFI systems the illumination and collection beams spatially overlap. Assuming the laser operates in the fundamental Gaussian mode, the measurement volume centred around the beam focus, is defined as the volume within which the optical intensity has a magnitude higher than  $1/e^2$  of the intensity peak value (Albrecht et al., 2003). Nevertheless, a very small particle in the measuring volume may not reflect sufficient light to be detected; therefore the detection volume in this case is smaller than the measurement volume. On the contrary, a large number of highly reflective particles may be detected, even if they are slightly outside the measurement volume as defined above. Under these conditions, the detection volume is clearly larger than the measurement volume. Throughout the article it is understood that the calculated measurement volume is only an estimate of the effective detection volume.

## 3 Experimental set-up

The laser used was a commercial VCSEL (Firecomms, model RVM665T) lasing at 667 nm with a threshold current,  $I_{\text{th}}$ , of 0.8 mA. In all experiments the VCSEL was operated at a constant current of  $2.25I_{\text{th}}$ , where it was found to exhibit good optical feedback sensitivity and stability, as well as single mode behaviour. A dual-lens system was used (Fig. 1) with collimating (lens 1) and focusing (lens 2) lenses of respective focal lengths 15.29 and 8 mm. The laser beam

axis was angled at  $80^\circ$  relative to the flow direction. The two lenses were chosen so as to minimize the spot size, and hence improve the spatial resolution of the measurement system. The assembled optical head was characterized with a beam profiler, and the spot diameter in focus was measured to be  $32.26 \mu\text{m}$ . This results in a sensing volume of  $7.16 \times 10^5 \mu\text{m}^3$ , providing for a sufficient spatial resolution to scan the channel, which has a  $320 \mu\text{m}$  internal diameter. The optical head was mounted on a computer controlled 3-axis motorized translation stage. The focus point was stepped through the channel by the translation stage to obtain the measurement points needed to reconstruct the flow profile.

The voltage across the VCSEL terminals was AC-coupled to a low-noise voltage amplifier and then fed into an analog-to-digital converter for digital signal processing on computer. A Fast Fourier Transform (FFT) was performed in software to obtain the signal frequency spectrum. All the reported Doppler spectra have been obtained as the mean of 64 successively acquired spectra. The acquisition time was lower than 10 ms. Therefore, the sensor response time can be considered as being close to real-time.

A microfluidic channel with circular cross-section of inner diameter  $320 \mu\text{m}$  was fabricated using Polydimethylsiloxane (PDMS) with the refractive index of 1.4 (Mark, 1999). The liquid under test was composed of 98 % water and 2 % milk by mass.

For a laminar flow, the velocity profile in a circular channel is parabolic, with the velocity increasing from zero at the wall (no slip boundary condition) to a maximum value at the centre. The Reynolds number, which indicates laminar regime is defined by:

$$Re = \frac{QD_H}{\nu A} \quad (2)$$

Where  $Q$  is the volumetric flow rate ( $\text{m}^3/\text{s}$ ),  $D_H$  is the hydraulic diameter (m),  $A$  is the pipe cross-sectional area ( $\text{m}^2$ ) and  $\nu$  is the kinematic viscosity ( $\text{m}^2/\text{s}$ ), that can be expressed by:

$$\nu = \frac{\mu}{\rho} \quad (3)$$

Where  $\mu$  is the dynamic viscosity of the fluid (Pa.s) and  $\rho$  is the density of the fluid ( $\text{kg}/\text{m}^3$ ). By assuming that the particle concentration in our solution is low enough that the parameters of the fluid can be approximated to those for water ( $\mu = 0.001 \text{ Pa.s}$ ,  $\rho = 997 \text{ kg}/\text{m}^3$  at  $20^\circ\text{C}$ ) and with respect to the flow rates imposed (from 5 to  $50 \mu\text{L}/\text{min}$ ), the Reynolds number varies from 0.33 to 33 (laminar regime).

The velocity profile in a circular cross-section channel for Newtonian fluid in the laminar regime is given by Poiseuille's law. In order to investigate non-Newtonian flow profiles, xanthan gum powder was added in various concentrations to

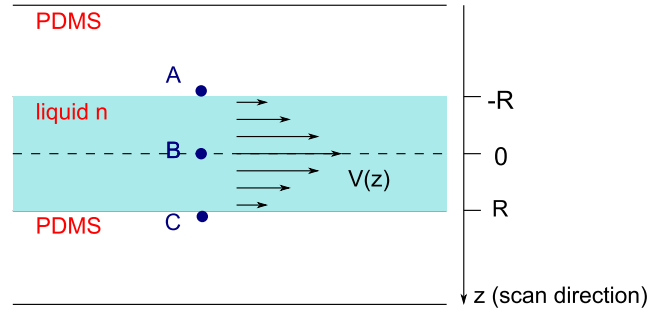


**Fig. 2** Diagram showing the scan configuration with respect to the  $z$ -axis of the flow channel. The angle calibration is calculated at position B, and the velocity profile is measured from A to C. The flow channel has a  $160 \mu\text{m}$  internal radius  $R$

the 2 % milk solution used previously. Xanthan gum, whose viscosity decreases with shear rate, shows a shear-thinning behaviour. The Ostwald-de-Waele law is chosen to model the variation of viscosity  $\mu$  with shear rate  $\dot{\gamma}$  for the xanthan gum based liquid phase:

$$\mu = K \cdot \dot{\gamma}^m \quad (4)$$

where  $K$  is the consistency index and  $m$  the flow index. They are determined from experimental rheograms. The analytical solutions for the velocity profile when a purely shear-thinning fluid flows inside a circular channel is given by:

$$V(z) = \frac{2Q}{S} \frac{3m}{m+1} \left( 1 + \left( \frac{z}{R} \right)^{\frac{m+1}{m}} \right) \quad (5)$$

where  $Q$  is the pumping flow rate,  $S$  the area of the cross-section of the channel,  $z$  the distance from the center, and  $R$  the radius of the channel.

## 4 Experimental Results

### 4.1 Sensor calibration

The sensor was calibrated using a solution of 98 % distilled water and 2 % milk. First, the laser beam focus was moved to the middle of the channel (position B in Fig. 2) and the position was then further adjusted to where the OFI signal exhibited the highest frequency (Fig. 3). Then, the average Doppler frequency within the sensing volume was extracted from the OFI signal spectrum using the following fitting function:

$$af^{-b} + c + d \exp \frac{-(f - f_{\text{peak}})^2}{h} \quad (6)$$

where  $a$ ,  $b$  and  $c$  are the fitting parameters depending only on the experimental set-up. Thus,  $a$  and  $b$  in the first term are the parameters used for fitting the  $1/f$  noise, and parameter  $c$  in the second term is used for fitting the broadband noise in the spectrum. In the last term of the fitting function,  $d$  corresponds to the strength of the Doppler peak, the half-width

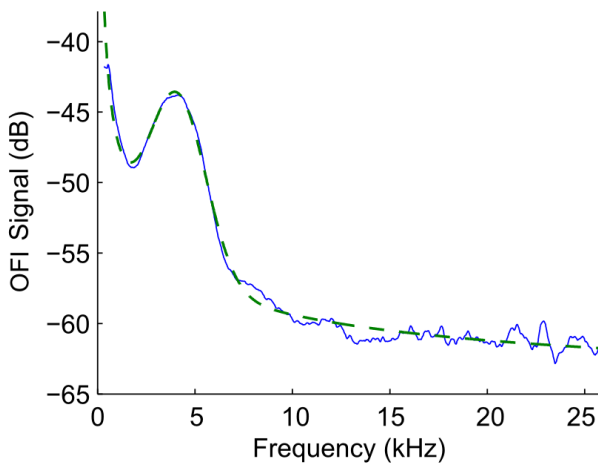


**Fig. 3** OFI signal in frequency domain measured at the middle of the channel and the corresponding fitting curve (Eq. (6)). The mean frequency in the sensing volume is calculated by extracting the Doppler frequency of the signal

at half maximum of the Doppler spectra being represented by  $h$ . The parameters  $d$ ,  $h$  and  $f_{\text{peak}}$  depend on the electro-optical system design, as well as on the reflectivity and the number density of particles, the fluid velocity, and the velocity distribution within the detection volume. The parameter  $f_{\text{peak}}$  represents the fluid velocity at the measurement point.

Doppler spectra were recorded at different fluid flow rates  $Q$  from 0 to 50  $\mu\text{L}\cdot\text{min}^{-1}$  (Fig. 4(a)). The frequency of the Doppler peak as a function of the maximum velocity  $V_{\text{max}} = \frac{2Q}{S}$  is shown in Fig. 4(b).

The final step of the calibration procedure consists in calculating the incident angle  $\theta$  from the slope of the fitting in Fig. 4(b). It was calculated to be  $80.25^\circ$ , close to the value given by the goniometer stage.

#### 4.2 Laminar flow profile : Newtonian fluid

To measure the velocity profile, the laser focus was first moved back to position A in Fig. 2, and the laser scanned across the flow channel ( $z$  direction in Fig. 2) in  $10\ \mu\text{m}$  steps toward position C.

The first liquid under test was milk diluted in distilled water (1:50), pumped at  $20\ \mu\text{L}\cdot\text{min}^{-1}$ , which corresponds to an average velocity of  $4.15\ \text{mm}\cdot\text{s}^{-1}$ . The experimentally reconstructed flow profile is plotted in Fig. 5. The solid curve represents the theoretical parabolic velocity profile described by Poiseuille's law, whereas the blue curve represents the measured velocity at each radial location. The experiment agrees well with theory in the mid to high flow rate range.

The difference between the experimental and the theoretical velocities is plotted in Fig. 6. Notwithstanding the

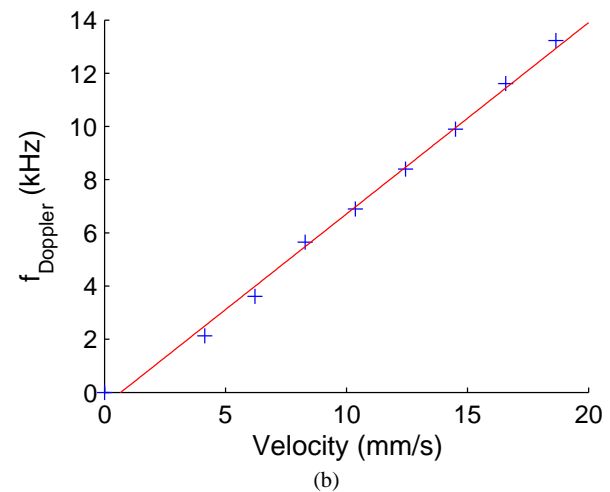
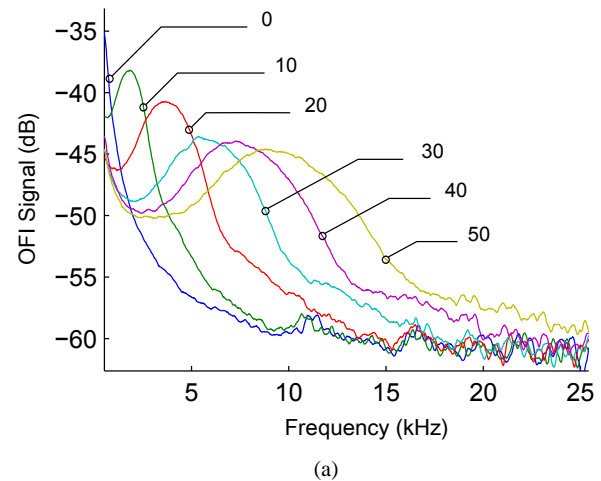


**Fig. 4** (a) OFI signal in the frequency domain for several flow rates (0, 10, 20, 30, 40 and 50  $\mu\text{L}\cdot\text{min}^{-1}$ ) (b) Plot of the Doppler frequency as a function of the flow rate. The peak frequency shows a linear relationship with velocity. The angle between the flow direction and the optical beam can be estimated from the slope of this relationship, and has been calculated to be  $80.25^\circ$

first point (with a discrepancy of 3 %), this measurement indicates good agreement with theory. Over the usable range, the relative error for each measurement point was less than 1.8 %. The error near the channel's walls can be attributed to the difficulty in fitting the Gaussian peak close to the low frequency noise induced by the system.

To estimate the repeatability of the measurement, the standard deviation for 8 consecutive scans was calculated for each measurement point (Fig. 5). In addition to the increase of the error observed in the previous paragraph, the sensor shows also a compromised repeatability near the channel's wall. The discrepancy observed at low particle velocities can be also explained by difficulties in extracting the Gaussian peak from low frequency noise. Nevertheless, overall this measurement indicates good repeatability.

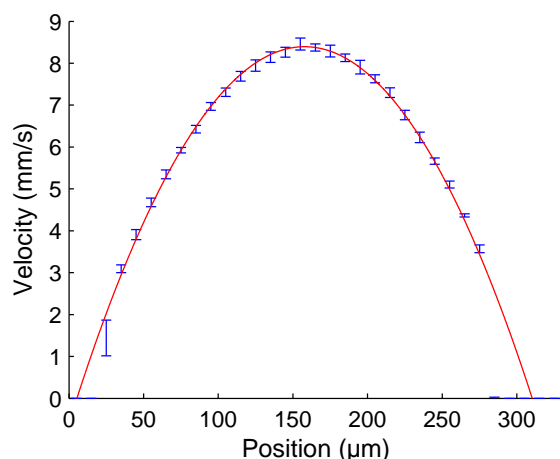


**Fig. 5** A comparison between theoretical profile (solid red curve) and 8 consecutive measured profiles (blue errorbars) along the centre-line of the flow channel with a flow speed of  $20 \mu\text{L}/\text{min}^{-1}$ . The liquid is milk (2 %) diluted in water

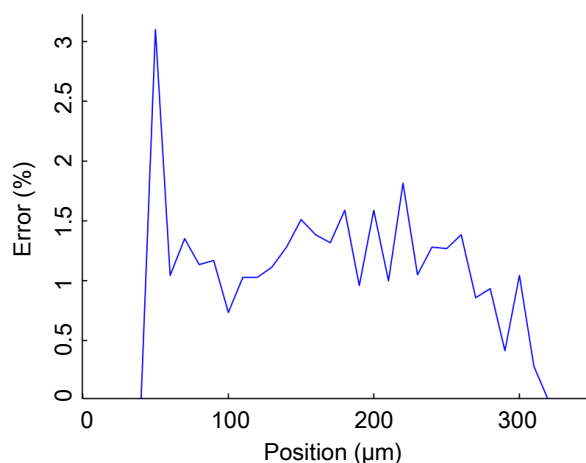


**Fig. 6** The mean measurement error to the theoretical profile as a function of the scanned position within the tube

The minimum spatial resolution of the system depends on the fluid composition and velocity, and could not be accurately measured. The laser spot size has been estimated at  $32 \mu\text{m}$ , but Fig. 5 and Fig. 8 show that the effective spatial resolution of the sensor is better than  $10 \mu\text{m}$ . These preliminary results demonstrate the feasibility of OFI measurement in microchannels of size well below  $320 \mu\text{m}$ . Future work shall consist in characterizing accurately the OFI spatial resolution as a function of the fluid parameters and the optical system.

#### 4.3 Laminar flow profile : Shear thinning fluid

Adding a shear thinning fluid to the initial milk-water mix leads to a different velocity distribution in microchannels.

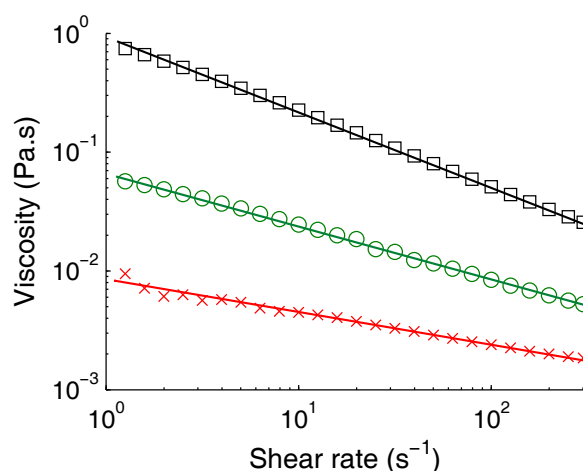


**Fig. 7** Experimental rheograms for various concentrations of xanthan gum (0.25 (cross) 1 (circle) and 3 g/L (square)). The viscosity of each solution as a function of the shear rate applied are plotted in logarithm

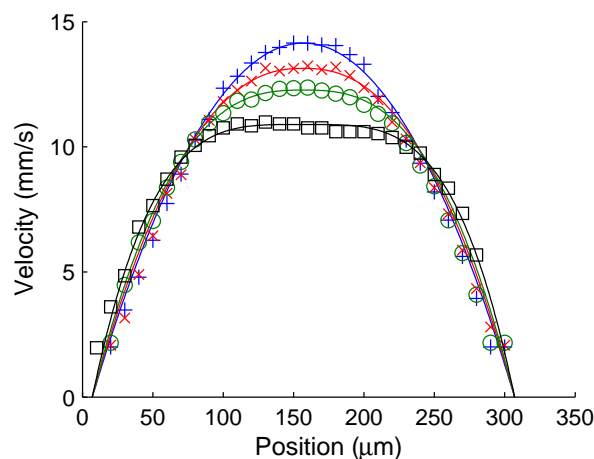


**Fig. 8** Measured (markers) and theoretical (solid line) velocity profile in a  $320 \mu\text{m}$  channel for various solutions of xanthan gum (0 (plus), 0.25 (cross), 1 (circle), and 3 g/L (square))

Within the laminar range, the velocity profile is expected to become flatter in the center as the solution becomes shear-thinning.

Four solutions at different xanthan gum concentrations (0, 0.25, 1, and 3 g/L) were pushed through the flow channel at a pumping rate of  $30 \mu\text{L}\cdot\text{min}^{-1}$ . We measured the relationship between the shear rate and the viscosity for each solution, using a rheometer (TA instruments AR 2000) in a small-angle cone and plate configuration (Fig.7). The temperature was controlled at  $25 \text{ }^\circ\text{C}$ . The power law exponent  $m$  was then extracted from these experimental rheograms using Eq. (4), and found to be 1, 0.73, 0.56, and 0.37 respectively. The theoretical velocity profiles are obtained using Eq. (5) and the calculated values of  $m$ , and are compared to the measurement results in Fig. 8. The experimental profile for non-Newtonian fluid in the laminar range shows also

good agreement with theory (Eq. 5). Thus the discrimination of different velocity profiles by OFI is demonstrated, and the technology's application to the measurement of complex flow behaviour is verified.

## 5 Conclusion

An OFI microfluidic flow sensor capable of accurately measuring flow rates and profiles in micrometer-scale channels was presented. Flow profile reconstruction of laminar flow in a channel with an internal diameter of 320  $\mu\text{m}$  was demonstrated. OFI differs from the well established technique of  $\mu\text{-PIV}$  by the simplicity of implementation and the low cost of its technology. The OFI sensors can be fully automated, offering opportunity of on-site implementation with unskilled operators. OFI possible applications include following the establishment of flow steady-state regime, detecting the deviations from normal behaviour, and performing rapid one dimensional flow scans.

However,  $\mu\text{-PIV}$  remains so far the most powerful tool to accurately measure fluid flow distribution in complex systems (multiphase flows, complex rheology..), and to provide velocity distribution in large two-dimensional areas.

Future extensions of this work include operation in the multiple scattering regime and characterization of non-laminar flows. Considering it is a single point raster-scanning technique (in its current implementation), OFI has limited applicability for mapping large flow-channels. Its demonstrated acquisition time is around 10 ms per single point measurement which effectively limits the image resolution achievable. Nevertheless, the use of a VCSEL array (Lim et al., 2009, 2010) can remove the need for mechanical scanning completely, thus improving acquisition time, spatial resolution and reducing mechanical complexity of the system. This should lead to the acquisition of a complete map of the velocity distribution in a channel in about 10 ms. Using OFI to characterize liquids through measurement of their flow profiles could lead to innovative, new, low-cost sensors, and brings about new possibilities for the design of enhanced Bio-system-on-a-Chip.

**Acknowledgements** This work was performed in part at the Queensland node of the Australian National Fabrication Facility, a company established under the National Collaborative Research Infrastructure Strategy to provide nano and microfabrication facilities for Australia's researchers. This research was supported under Australian Research Council's Discovery Projects funding scheme (DP0988072), and The Commonwealth of Australia International Science Linkages programme (FR090026)

## References

- Ahmed, B., Barrow, D., and Wirth, T. (2006). Enhancement of reaction rates by segmented fluid flow in capillary scale reactors. *Advanced Synth. & Catalysis*, 348(9):1043–1048.
- Albrecht, H.-E., Borys, M., Damaschke, N., and Tropea, C. (2003). *Laser Doppler and Phase Doppler Measurement Techniques*. Springer Verlag, Berlin.
- Anxionnaz, Z., Cabassud, M., Gourdon, C., and Tochon, P. (2008). Heat exchanger/reactors (hex reactors): Concepts, technologies: State-of-the-art. *Chem. Eng. and Proc. : Process Intensification*, 47:2029–2050.
- Bosch, T., Bes, C., Scalise, L., and Plantier, G. (2006). Optical feedback interferometry. In Grimes, C. A., Dickey, E. C., and Pishko, M. V., editors, *Encyclopedia of Sensors*, volume X, pages 1–20. American Scientific Publishers, Valencia, CA.
- de Groot, P. and Gallatin, G. (1989). Backscatter-modulation velocimetry with an external-cavity laser diode. *Opt. Lett.*, 14(3):165–167.
- de Mello, A. and Wooton, R. (2002). But what is it good for? applications of microreactor technology for the fine chemical industry. *Lab Chip*, 2:7N–13N.
- de Mul, F., Koelink, M., Weijers, A., Greve, J., Aarnoudse, J., Graaff, R., and Dassel, A. (1992). Self-mixing laser-doppler velocimetry of liquid flow and of blood perfusion in tissue. *Appl. Opt.*, 31(27):5844–51.
- Giuliani, G., Norgia, M., Donati, S., and Bosch, T. (2002). Laser diode self-mixing technique for sensing applications. *J. of Opt. A: Pure and Appl. Opt.*, 4(6):283–294.
- Kane, D. M. and Shore, K. A., editors (2005). *Unlocking Dynamical Diversity: Optical Feedback Effects on Semiconductor Lasers*. John Wiley.
- Kliese, R., Lim, Y. L., Stefan, E., Perchoux, J., Wilson, S., and Rakic, A. (2010). Rapid scanning flow sensor based on the self-mixing effect in a vcsel. In *Conf. on Optoelectron. and Microelectron. Mater. and Devices (COM-MAD)*, pages 7–8.
- Lim, Y. L., Kliese, R., Bertling, K., Tanimizu, K., Jacobs, P. A., and Rakic, A. D. (2010). Self-mixing flow sensor using a monolithic vcsel array with parallel readout. *Opt. Expr.*, 18(11):11720–11727.
- Lim, Y. L., Nikolic, M., Bertling, K., Kliese, R., and Rakic, A. D. (2009). Self-mixing imaging sensor using a monolithic vcsel array with parallel readout. *Opt. Expr.*, 17(7):5517–5525.
- Mark, J. E. (1999). *Polymer Data Handbook*. Oxford University Press.
- Meinhart, C. D., Wereley, S. T., and Santiago, J. G. (1999). Piv measurements of a microchannel flow. *Exper. in Fluids*, 27:414–419.

- Norgia, M., Pesatori, A., and Rovati, L. (2010). Low-cost optical flowmeter with analog front-end electronics for blood extracorporeal circulators. *IEEE Trans. on Instrum. and Meas.*, 59(5):1233–1239.
- Norgia, M., Pesatori, A., and Rovati, L. (2012). Self-mixing laser doppler spectra of extracorporeal blood flow: A theoretical and experimental study. *IEEE Sens. J.*, 12(3):552–557.
- Santiago, J. G., Wereley, S. T., Meinhart, C. D., Beebe, D. J., and Adrian, R. J. (1998). A particle image velocimetry system for microfluidics. *Exper. in Fluids*, 25:316–319.
- Sarrazin, F., Loubire, K., Prat, L., Gourdon, C., Bonometti, T., and Magnaudet, J. (2006). Experimental and numerical study of droplets hydrodynamics in microchannels. *AIChE*, 52:4061–4070.
- Zakian, C., Dickinson, M., and King, T. (2005). Particle sizing and flow measurement using self-mixing interferometry with a laser diode. *J. of Opt. A: Pure and Appl. Opt.*, 7(6):445–452.